

# Simultaneous evaluation of multiple microarray surface chemistries through real-time interferometric imaging

Chiodi E.\*<sup>(1)(2)</sup>, Sola L.<sup>(1)</sup>, Brambilla D.<sup>(1)</sup>, Marn A.<sup>(2)</sup>, Unlu S.<sup>(2)</sup>, Chiari M.<sup>(1)</sup>

(1) Institute of Chemistry of Molecular Recognition  
National Research Council of Italy  
Via Mario Bianco 9  
20131 Milan Italy

(2) Boston University  
Department of Electrical Engineering  
Photonics Center  
8, St. Mary's Street  
02215 Boston (MA) USA

*\*To whom correspondence should be addressed:*

Dr. Elisa Chiodi

e-mail: [elich@bu.edu](mailto:elich@bu.edu)

telephone: +1 617-206-0221

**Keywords:** IRIS; Interferometric Reflectance Imaging Sensor; functional polymers; polymer spotting; localized surface functionalization; microarray; binding kinetics;

**Abstract:** Surface chemistry is one of the most crucial aspects for microarray modality biosensor development. As a matter of fact, the immobilization capability of the functionalized surface is one of the limiting factors for the final yield of the binding reaction. In this work, we locally functionalized many reactive polymers on a single solid support allowing for a direct comparison of functionality of probes immobilized on different polymers and demonstrating a new way of multiplexing in which immobilization for each molecular probe can be individually optimized. Our goal was to investigate the immobilization efficiency of reactive polymers, as well as the resulting affinity of the molecular probes, in a single experiment. This idea was demonstrated by spotting a large number of different reactive polymers on an untreated Si/SiO<sub>2</sub> chip, and depositing the same molecular probe on all the spots immediately after. This method proved to be efficient and it could be used as an initial qualitative assay to decide which functionalization better suits a certain application, as opposed to flat-coating numerous different substrates and comparing them, which is time-consuming and expensive. We also showed that the localized functionalization method is applicable to proteins as well as oligonucleotides. Moreover, by means of real-time dynamic binding measurements performed with the Interferometric Reflectance Imaging Sensor (IRIS), we demonstrated that this newly-developed functionalization technique is comparable to the uniformity of classical flat-coating solution, both for the amount of immobilized biomaterial and for maintaining a similar affinity of the spotted probes. Indeed, the comparison between the binding curves that were obtained from different polymer spots with the same probe allowed us to decide which polymers would work better to immobilize a model protein,  $\alpha$ -lactalbumin, both native and a DBCO-modified variant. We corroborated our findings by performing similar IRIS experiments with two of the previously tested polymers in a classic flat-coating configuration and proving that the results are comparable. The final outcome is promising and it highlights the multiplexing power of this method: first, it allows to characterize dozens of polymers at once, within a single 60-minutes experiment. Secondly, it removes the limitation, related to coated surfaces, that only molecules with the same functional groups can be tethered to the same support - and therefore studied at the same time. By applying this innovative protocol, there is no more restriction on the type of molecules that can be studied simultaneously and immobilization for each molecular probe can be individually optimized.

## 1. Introduction

Microarrays are analytical devices that work by allowing specific binding between target probes immobilized on the surface (namely, spots) and analyte molecules in solution [1]. Since microarray-based assays were first introduced in 1995 [2], they have rapidly gained popularity in various biological research areas, due to their multiplexing capability and small volume requirement.

The effectiveness of a microarray-based experiment mostly depends on how the probe molecules are immobilized on the surface. As a matter of fact, the immobilization method chosen influences the stability of the molecules as well as their reactivity. For example, if the ligand is not stably bound, it may be lost throughout the experiment. On the contrary, if the probe is immobilized too tightly, it may be less flexible or lose its structure, and therefore have less sites available for binding.

Coating the slide surface with a hydrophilic polymer prior to spotting allows to create a uniform, homogeneous, thin, reactive layer on which the molecules can be immobilized as far from the surface as necessary for them to remain active.

In the last ten years, our group has introduced a family of N, N-dimethylacrylamide (DMA) based polymers that form a thin film on different materials by a combination of physi and chemisorption [3]. In an effort to tailor surface properties, the precursor of this polymer family, a copolymer of dimethylacrylamide with N-Acryloyloxysuccinimide (NAS) and 3-(Trimethoxysilyl)propyl methacrylate (MAPS), has been modified with several building blocks to introduce, for example, azide, alkyne, dibenzocyclooctine, maleimide, functionalities thanks to the reactivity of NAS with amino-groups [4]. The introduction of other functional groups by post polymerization modification (PPM) reactions and the combination of different monomers during the synthesis has allowed to generate many polymers, ten of which were used in this work (see Fig. 1 and Table 1 for monomer mole percent). All these polymers share a common backbone of DMA and MAPS which confer them adhesive properties on a variety of surfaces.

The classical dip and rinse coating approach used with these polymers requires immersing the substrate in their aqueous solution followed by rinse and dry steps [5]. Thanks to the adhesive properties of the polymers, this approach, that is considerably simpler than most of the approaches used to produce polymeric coatings, was further simplified by localizing the coating through the spotting of only ultra-small amount of polymer. Theoretically, dozens of different polymers could be arrayed on the surface, thus creating a number of different interfaces between the surface and the probes. Considering how many polymers are available and how differently they react with each

probe, deciding which surface chemistry is the optimal one for every experiment is time consuming and laborious, as well as expensive. Indeed, the classical method would include coating many different slides with the different polymers one is willing to test, spotting each of them and perform measurements on them separately. This process results in a copious use of reagents, it is time-consuming and it may as well cause a non-trivial amount of statistical noise due to the experimental conditions that inevitably change for every experiment - for example, subtle changes in the temperature or in the pH of the solutions.

In this work we combine the new approach for the immobilization of biomolecules based on the spotting pL amounts of aqueous solutions of the various copolymers, followed by the deposition on the same spot of the biomolecule to be immobilized [6] with a new real-time binding detection method [12] recently introduced by our group. This strategy provides an easy, inexpensive and quick assay to test the influence of surface properties on binding affinity in tiny areas on which each probe is anchored on a chemically different environment in a single 60-minutes experiment.

## 2. Material and methods

### 2.1 Materials

N,N-Dimethylacrylamide (DMA), 3-(trimethoxysilyl)propyl methacrylate (MAPS), 1H,1H,2H,2H-perfluorodecyl acrylate (PFDA),  $\alpha,\alpha'$ -Azoisobutyronitrile (AIBN), Acrylamido buffer pKa 3.6, acrylamido buffer pKa 8.5, dibenzocyclooctyne-N-hydroxysuccinimidyl ester (DBCO-NHS ester), anhydrous tetrahydrofuran (THF), petroleum ether, dimethylsulfoxide (DMSO), ammonium sulphate ( $(\text{NH}_4)_2\text{SO}_4$ ), phosphate buffered saline (PBS), sucrose monolaurate, Amicon Ultra centrifugal filters (MWCO 3K) and  $\alpha$ -Lactalbumin were purchased from Sigma Aldrich (St. Louis, MO, USA). Anti  $\alpha$ -Lactalbumin antibody was purchased from Abcam (Cambridge, UK). All solvents were used as received. N-acryloyloxysuccinimide (NAS) and 3-azido-1-propylamine were synthesized as reported elsewhere ([7],[8]).

Untreated silicon slides with 110 nm thermal grown oxide were supplied by Silicon Valley Microelectronics (Santa Clara, CA, USA).

Spotting was performed using a SciFLEXARRAYER S12 (Scienion, Berlin, Germany).

### 2.2 Polymer synthesis

All polymers, schematically represented in Fig.1, were synthesized as previously reported ([9],[10],[11]). Briefly, a 20% w/v total monomer concentration solution was prepared by dissolving each monomer (following the molar ratios reported in Table 1) in anhydrous THF. The solution was degassed for 20 min by purging argon into the monomer solution and then 2mM of a thermoinitiator (AIBN) was added. The solution was heated for 2 h at 65°C and kept under argon atmosphere. The solution was then diluted 1:1 with anhydrous THF and precipitated in petroleum ether (10 times the volume of the reaction mixture). Polymers were collected as a white powder, and dried under vacuum at room temperature.

Polymers containing charged groups were synthesized using acrylamido derivatives with carboxyl or tertiary amino side chains. These monomers are commercially available under the trade name of Acrylamido Buffer. The pKa of their ionizable groups covers the entire pH scale. The Acrylamido buffer with pKa 3.6 was used for the negative polymer, while the one with pKa 8.5 was chosen for the positive polymer. To synthesize amphoteric polymer, a mixture of these acrylamido buffers was used.

Azide functionalities were introduced in parent polymers containing N-Acryloyloxy succinimide (NAS) via post-polymerization modification, as described elsewhere [11]. Essentially the copolymer was dissolved in anhydrous THF to a final concentration of 20% w/v; a 2.5 molar excess, respect to the molar ratio of NAS, of 3-azido-1-propylamine was added to the crude material. The mixture was stirred for 5 h at room temperature under argon atmosphere and then diluted 1:1 with anhydrous THF. The polymers were precipitated in petroleum ether (10 times the volume of the reaction mixture), filtered on a Buchner funnel and dried under vacuum at room temperature.

**Figure 1:** Chemical structure of tested copolymers.

**Table 1:** Molar ratio of monomers used to synthesize polymers.

### 2.3 Synthesis of DBCO-modified $\alpha$ -Lactalbumin

3.53  $\mu$ L of 40 mM solution of DBCO-NHS ester in DMSO (10 equivalents) were added to 100  $\mu$ L of 1 mg/mL  $\alpha$ -Lactalbumin in PBS and allowed to react for 30 min at room temperature. At the end, 10  $\mu$ L of TRIS-HCl 1M pH8 were added to quench the reaction. After 5 min of quenching, the reaction mixture was filtered on Amicon Ultra 3K centrifugal filter for 2 min at 12,000xg to remove unreacted DBCO-NHS ester. PBS was finally added to the DBCO-modified  $\alpha$ -Lactalbumin solution to a final volume of 100  $\mu$ L, and the solution was deposited on silicon slides without further purification.

### 2.4 IRIS system

The Interferometric Reflectance Imaging Sensor (IRIS) uses optical phase difference to detect very small amounts of biomass that accumulate on an active surface (Figure 2). The setup is fully described in [12]. Briefly, the active surface is composed of a silicon chip with a thermally grown 110nm  $\text{SiO}_2$  layer; the chip contains two drilled through holes (Potomac) to allow the passage of liquid across the active surface. When the chip is illuminated from the top with a coherent source, the layered substrate creates a common path interferometer. By measuring the reflectance from the substrate at distinct wavelengths across the visible spectrum, we are able to reconstruct the reflectance curve from the layered substrate. Changes in the optical path length due to the capture of a target of interest on the  $\text{SiO}_2$  layer causes a measurable shift in this reflectance curve.

In our system, the sample can be illuminated by four independent LEDs with a peak at four different wavelengths (455 nm, 518 nm, 598 nm and 635 nm). However, continuously acquiring images with each of these four illumination wavelengths throughout the experiment, and then calculating the

reflectance curve for each four-color acquisition is computationally heavy and slow. Therefore, we start from the assumption, detailed in [13], that during the whole experiment the thickness varies in such a small range ( $\pm 10\text{nm}$ ) that it can be linearly correlated to the change in reflectivity. This way, we can acquire one single image in each of the four available LEDs at the beginning of the experiment, calculate the reflectance curve, and then use the resulting reflectance curve to create a look-up table for the conversion from reflectance to biomass thickness.

The images were acquired with a simple CCD camera (PointGrey) and analyzed through a custom-made ImageJ plugin and a MATLAB software. More details about the conversion from reflectance values to mass density can be found in [14].

Figure 2: The IRIS setup (..)

## 2.5 Chip surface functionalization

The experiments were performed on 25x12.5mm silicon chips (Fig. 3a), purchased from Silicon Valley Microelectronics (Santa Clara, CA) with a 110nm layer of silicon oxide grown on top. Chips were spotted with a SciFlexArrayer S12 spotter (Scenion, Berlin, Germany). First, polymer solutions were prepared by diluting them up to 0.014% in water with sucrose monolaurate 0.01% w/v, Then, 400 pL of either native or DBCO modified  $\alpha$ -lactalbumin 1mg/mL were spotted on top of that. The spotted chips were left overnight in a NaCl saturated humid chamber. The chips were washed with a 0.5 % w/v water solution of a copolymer of dimethylacrylamide and allyl glycidyl ether (EPDMA) synthesized as reported in [15]. This polymer, originally developed to suppress electroosmotic flow in capillary electrophoresis is known for its ability to form a thin layer on glassy surface with antifouling properties by dip and rinse approach.

Some experiments for this work were also performed in a flat coating configuration. For these experiments, the samples were prepared in a different way. Briefly, the surface of the chips was first oxygen plasma activated for 10 minutes and then the chips were immersed in the aqueous polymer solutions (1%, w/v polymer in an aqueous solution of 20% saturated ammonium sulfate) for 30 minutes. Afterwards, the substrates were washed with DI water and dried under nitrogen stream. Finally, to complete the coating procedure, they were baked in a stove at 80°C for 15 minutes. The chips were then spotted with 400pL of native  $\alpha$ -lactalbumin 1mg/mL. As above, the spotted chips were left overnight in a NaCl saturated humid chamber. However, in this case, a one-hour blocking step with a 50mM ethanolamine solution was performed to inactivate the residual amine groups on the surface.

## 2.6 Microfluidic chamber

Prior to starting the experiment, every chip (Figure 3a) was topped with an adhesive spacer and an AR coated glass slide to form a chamber for in-liquid measurements. The glass was purchased from Abrisa Technology (Torrance, CA) while the spacer was customized for us by Grace BioLabs (Bend, OR). The volume of the chamber obtained this way was less than 5uL. The whole system has a dead volume of less than 500uL.

**Figure 3: The chips (a) and the microfluidic chamber (b) used for IRIS measurements.**

## 3. Results and discussion

### 3.1 Localized surface functionalization: testing many surface chemistries on the same chip

The adhesive characteristics of DMA, MAPS copolymers allow to generate films on localized regions of the substrate by spotting pL amounts of polymer solutions. Two sets of polymers were used in this experiment: one contains succinimide esters while the second one contains azide groups. In each series, three variants were generated by copolymerizing, in addition to the backbone monomers, acrylic monomers bearing carboxyl or tertiary amine groups or a mixture of both monomers in such a ratio to define a precise isoelectric point. At the pH used for the hybridization, the surface is negatively or positively charged in the first two cases. The net charge of the amphoteric surface can be tuned from negative to positive depending on the pH of the hybridization buffer. In the experimental conditions used here it has an overall negative charge. In addition, the charge can be modulated by tailoring the ratio of the two acrylamido buffers in the polymer or by selecting different acrylamido buffers pairs.

The parent polymers, Copoly NAS 10% and its derivative Copoly Azide are neutral or only negligibly charged, they bind either native proteins by nucleophile reaction between succinimidyl esters and amino groups naturally present in proteins, or DBCO modified proteins by azide-alkyne strain promoted cycloaddition, a classical click chemistry reaction.

As mentioned above, the immobilization technique detailed here offers a set of advantages. First of all, it allows the user to save time by avoiding the whole time-taking process of coating the slide. Moreover, a much smaller quantity of polymer is needed with respect to flat-coating. Finally, a single experiment can provide information on the performance of multiple surface chemistries at a time.

In Figure 4 a schematic representation of the functionalization is reported. In a single spotting section, aqueous solutions of ten polymers at 0.014% w/v are spotted in array format. On top of each polymer the same protein,  $\alpha$ -lactalbumin (either native or DBCO-modified) at a concentration of 1 mg/mL is deposited. To avoid non specific adsorption of biomolecules on the area surrounding the spots, after deposition of the capture probe, a blocking step was performed using a hydrophilic polymer, EPDMA, previously reported by our group [15].

Figure 4 - Spotted polymers technique (a) and flat coating technique (b).

Figure 5 – Dry IRIS chip image acquired before starting the real-time binding experiment. On the chip a 6x6 matrix of  $\alpha$ -lactalbumin spots is visible. Each group of three spots corresponds to a different polymer.

The chip was used to run a 60-minutes long in-liquid IRIS experiment. First, filtered PBS buffer was flowed into the chamber for 15 minutes, allowing the system to stabilize. Afterwards, anti- $\alpha$ -lactalbumin antibody at 1ug/mL ( $\approx$ 7nM) was injected for 20 minutes at an average speed of 200uL/min. PBS buffer was then injected as a washing buffer for another 20 minutes. Finally, the surface was restored by flowing a 100 mM glycine buffer at pH=2 for 5 minutes. During this whole experiment, interferometric images were acquired. Each point of the curve in Fig. 6 corresponds to one acquired image. To get a better signal-to-noise ratio, each image is the average of 100 acquired frames.

Figure 6 - Anti-  $\alpha$ -lactalbumin binding to two different modifications of  $\alpha$ -lactalbumin spotted on a single IRIS chip. The solid lines in the inset (a) show a classic Langmuir fit of the data.

By analyzing the first 20 minutes of data, as detailed in par. 2.2, the binding curves in fig. 6a were obtained. A simple Langmuir one-to-one binding equation was used to fit the data (eq.1).

$$dm(t) = m_0 \cdot \frac{k_{ONC}}{k_{ONC} + k_{OFF}} \cdot (1 - e^{-(k_{ONC} + k_{OFF}) \cdot t}) \quad (\text{eq. 1})$$

This way, we could estimate the dynamic constants of the reactions. The parameters obtained from this analysis are reported in Table 2.

Table 2: ON and OFF rates obtained through a classic Langmuir fit of anti-  $\alpha$ -lactalbumin binding on different  $\alpha$ -lactalbumin modifications, spotted on top of different polymers spots.

As it can be noticed from Figure 6, the two families of polymers are clearly distinct in terms of dynamic behavior and equilibrium points reached.

However, this preliminary result mainly depends on the mass density value at the beginning of the experiment – that is, the immobilized biomaterial that remains on the surface after spotting.

Indeed, a significant correlation exists between the equilibrium point reached by each curve and the average initial mass per spot (Table 3).

**Table 3:** Initial mass density values for the different polymers spots.

To quantitatively understand this correlation, we calculated the correlation coefficient between the initial mass on the surface and the equilibrium points reached, as in equation 2:

$$\rho_{m_0, m_{eq}} = \frac{cov(m_0, m_{eq})}{\sigma_{m_0} \cdot \sigma_{m_{eq}}} \quad (\text{eq.2})$$

This calculation led to a correlation coefficient value of 0.85, which can be considered significant.

**Figure 7 –** Correlation between the initial mass density value and the equilibrium value reached by the antibody binding to different polymer spots.

Measuring how much mass the polymers immobilized is both interesting and informative, and we did so with DNA in our previous work on this topic [6]. However, another really important data we are interested in is how reactive the immobilized molecules are. A good approach would be to normalize the curves above by dividing them for the initial mass value (fig. 8).

**Figure 8:** The curves in figure 6a, normalized by dividing every curve for the initial mass value.

This normalization shows that having a large quantity of biomaterial immobilized on the surface is not always a good indication of the high reactivity of the probes. Indeed, even if the overall binding is higher on the Copoly Azide 10% amphoteric spot (figure 2), in the end the neutral Copoly Azide spot almost doubles its mass density ( $m/m_0 \approx 1$ , figure 3), while the former accumulates less than half of the initial mass value ( $m/m_0 \approx 0.5$ ). A possible explanation for this is that the presence of charges could inhibit the binding of this specific antibody due to electrostatic repulsion. Another possibility is that the charged polymers immobilize the probe so tightly that they modify its structure

and therefore affect its reactivity. This second possibility is less probable, since  $\alpha$ -lactalbumin is quite symmetric and the charges are well distributed on its surface. (Matt? Model?)

To summarize, even though the neutral polymers retain less mass from spotting (Table 3, Figure 6) the molecules that are immobilized onto those show a higher reactivity (Fig. 8).

### 3.2 Comparison to flat coating

To further demonstrate that our assay is comparable to the classical flat-coating method, in terms of qualitative performance of the polymers, we chose two of the polymers mentioned above, namely Copoly NAS 10% amphoteric and Copoly Fluoride, and we performed the same measurements in a flat coating configuration.

First, two chips were coated with, respectively, Copoly Fluoride and Copoly NAS 10% amphoteric, with the classical flat coating procedure as described in the Material and Methods section (Par. 2.3).

Figure 9 – Dry IRIS chip images acquired before starting the real-time binding experiment. (a) Copoly-10F coated chip and (b) MCP-4 amphoteric coated chip. On both a 6x6 matrix of  $\alpha$ -lactalbumin spots is visible.

On both chips, the same IRIS experiment described above was performed: the chamber was mounted, with the glass and spacer, and the obtained cartridge was positioned inside the instrument. PBS buffer was flowed into the chamber for 15 minutes to stabilize the system. Afterwards, anti  $\alpha$ -lactalbumin 1ug/mL ( $\approx$ 7nM) was injected and recirculated for 20 minutes at an average speed of 200uL/min. A 20-minutes washing with PBS was performed and a 5-minutes surface restoration with a 100mM glycine solution (pH=2) was used to go back to the starting point.

Figure 10: Anti-alpha-lactalbumin binding to  $\alpha$ -lactalbumin spotted on two flat-coated IRIS chips: one coated with Copoly Fluoride (light blue curve) and one with Copoly NAS 10% Amphoteric (yellow). The solid lines in the inset (a) show a classic Langmuir fit of the data.

Table 4: ON and OFF rates obtained through a classic Langmuir fit of anti-  $\alpha$  -lactalbumin binding on spotted Copoly Fluoride (blue curve, fig.4a) and on spotted Copoly NAS 10% amphoteric (yellow curve, fig.4a).

As for the experiment described in Paragraph 3.1, every point of the curves displayed in Figure 10 corresponds to the average of 100 acquired frames.

The parameters (Table 4) and the curves (Figure 10) obtained show that these two polymers qualitatively behave the same in both configurations. Indeed, by comparing Fig.6 and Fig. 9, one can notice that in both cases the equilibrium point reached by the Copoly Fluoride curve is sensibly lower than the one reached by Copoly NAS 10% amphoteric.

**Table 5 – Comparison of the initial mass density value for Copoly Fluoride and Copoly NAS 10% amphoteric polymers for the two experiments.**

Moreover, one can compare the initial mass values in the two cases (Table 5) and observe that they are in good agreement.

To investigate the problem in depth, we normalized these data the same way we did above, by dividing the curves for the initial mass value (Fig. 11). The result confirmed the previous findings: the two polymers behave the same way in terms of reactivity, as it emerges also from the data in Fig. 8, where the light blue curve (Copoly Fluoride) is following the same path as the green one (Copoly NAS 10% amphoteric).

**Figure 11:** The curves in Figure 10, normalized by dividing each of them by the initial mass density value.

#### 4 Conclusions

In summary, we pursued the effort we started in our latest work [6] of developing an innovative assay that allows to simultaneously test the performance of different surface chemistries, localized on distinct regions of the same support. Most importantly, we demonstrated that this immobilization technology can successfully be applied to proteins as well as oligonucleotides, which is not trivial and could be challenging due to the complexity of protein structure. Following the path started in [6], we precisely quantified both the initial mass immobilized on each localized polymer spot as well as the final yield of the reaction. Moreover, we calculated the correlation between those values and, thanks to the real-time binding measurements, we could estimate the actual reactivity of the probes by applying a simple normalization. A single 60-minutes experiment was therefore enough to collect all the information that is necessary to qualitatively compare the performance of the different polymers. The results were in optimal agreement with those obtained in the classical flat-coating configuration. We therefore showed that the combination of this localized functionalization technology and the real-time, in liquid IRIS technique allows the user to quickly understand which surface chemistry would better suit any specific application. Furthermore, it removes the limitation regarding the number of molecules with different chemistries that can be immobilized on the same support.

#### 4 References

- [1] MacBeath G.: Protein microarrays and proteomics. *Nature Genetics*, 32 (Suppl.), 526-532 (2002) <http://doi.org/10.1038/ng1037>
- [2] Schena M., D. Shalon, R. W. Davis, and P. O. Brown: Quantitative monitoring of gene expression patterns with a complementary DNA microarray. *Science*, 270, 467-470 (1995) <http://doi.org/10.1038/ng1037>
- [3] Pirri, G., Damin, F., Chiari, M., Bontempi, E., and Depero, L. E. (2004) Characterization of A Polymeric Adsorbed Coating for DNA Microarray Glass Slides. *Anal. Chem.* 76, 1352–1358.
- [4] Sola, L., Damin, F., Gagni, P., Consonni, R., and Chiari, M. (2016) Synthesis of clickable coating polymers by postpolymerization modification: Applications in microarray technology. *Langmuir* 32, 10284–10295.
- [5] Zilio, C., Sola, L., Damin, F., Faggioni, L., and Chiari, M. (2014) Universal hydrophilic coating of thermoplastic polymers currently used in microfluidics. *Biomed. Microdevices* 16, 107–114.
- [6] Sola, L., Damin, F., Chiari, M., Array of multifunctional polymers for localized immobilization of biomolecules on microarray substrates, ANALYTICA CHIMICA ACTA, 2019, Volume: 1047, Pages: 188-196
- [7] M. Mammen, G. Dahmann, G.M. Whitesides, Effective inhibitors of hemagglutination by influenza virus synthesized from polymers having active ester groups. Insight into mechanism of inhibition, *J. Med. Chem.* 38 (1995) 4179e4190, <https://doi.org/10.1021/jm00021a007>.
- [8] F. Landi, C.M. Johansson, D.J. Campopiano, A.N. Hulme, Synthesis and application of a new cleavable linker for “click”-based affinity chromatography, *Org. Biomol. Chem.* 8 (2010) 56e59, <https://doi.org/10.1039/b916693a>.
- [9] L. Sola, M. Chiari, Modulation of electroosmotic flow in capillary electrophoresis using functional polymer coatings, *J. Chromatogr. A* 1270 (2012) 324:329, <https://doi.org/10.1016/j.chroma.2012.10.039>.
- [10] L. Sola, F. Damin, M. Cretich, M. Chiari, Novel polymeric coatings with tailored hydrophobicity to control spot size and morphology in DNA microarray, *Sensor. Actuator. B Chem.* 231 (2016), <https://doi.org/10.1016/j.snb.2016.03.049>.
- [11] L. Sola, F. Damin, P. Gagni, R. Consonni, M. Chiari, Synthesis of clickable coating polymers by post-polymerization modification: application in microarray technology, *Langmuir* 32 (2016) 10284e10295.
- [12] Ozkumur E., Needham J. W., Bergstein D. A., Gonzalez R., Cabodi M., Gershoni J. M., Goldberg B. B., Unlu M. S.: Label-free and dynamic detection of biomolecular interactions for high-throughput microarray applications. *Proceedings of the National Academy of Sciences of the United States of America*, 105, 7988–7992 (2008).

<http://doi.org/10.1073/pnas.0711421105>

[13] Sevenler D., Ünlü M.S.: Numerical techniques for high-throughput reflectance interference biosensing. *Journal of Modern Optics*, **63**, 1115–1120 (2016).

<http://doi.org/10.1080/09500340.2015.1117668>

[14] Ozkumur E., Yalçın A., Cetin M., Lopez C., Bergstein D., Goldberg B. B., Chiari M., Ünlü M. S.: Quantification of DNA and protein adsorption by optical phase shift. *Biosensors and Bioelectronics*, **25**, 167–172 (2009).

<http://doi.org/10.1016/j.bios.2009.06.033>

[15] Chiari., M., Cetin., M., Damin., F., Ceriotti., L., Consonni., R., New adsorbed coatings for capillary electrophoresis, *Electrophoresis*, 2000, 21, 909-916.

## Figures:

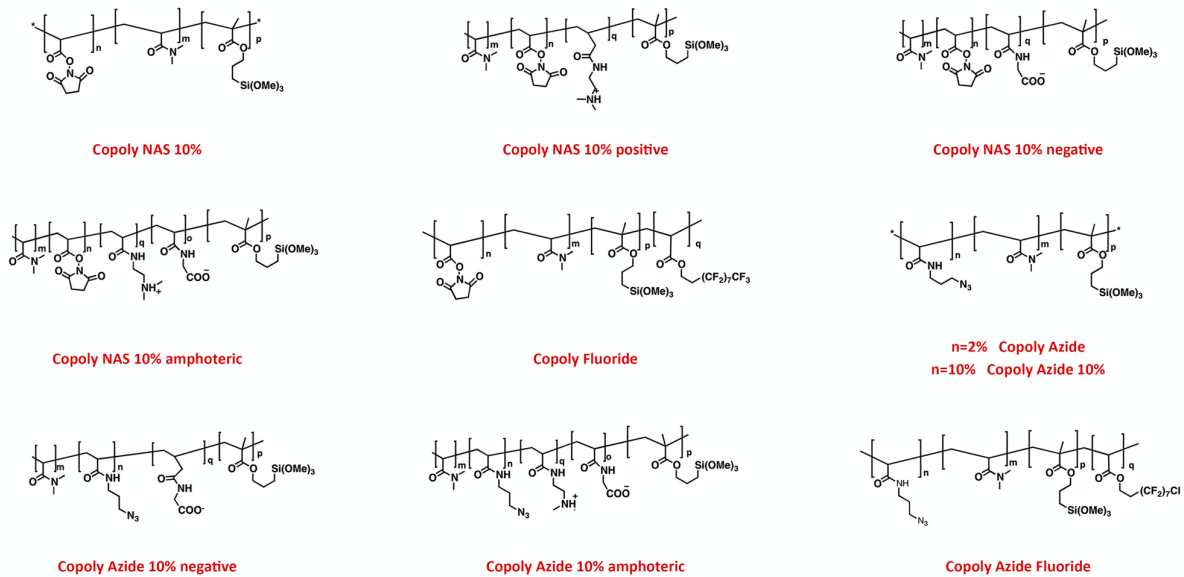


Figure 1: Chemical structure of tested copolymers.

Figure 2: The IRIS setup (..)

Figure 3: The chips (a) and the microfluidic chamber (b) used for IRIS measurements.

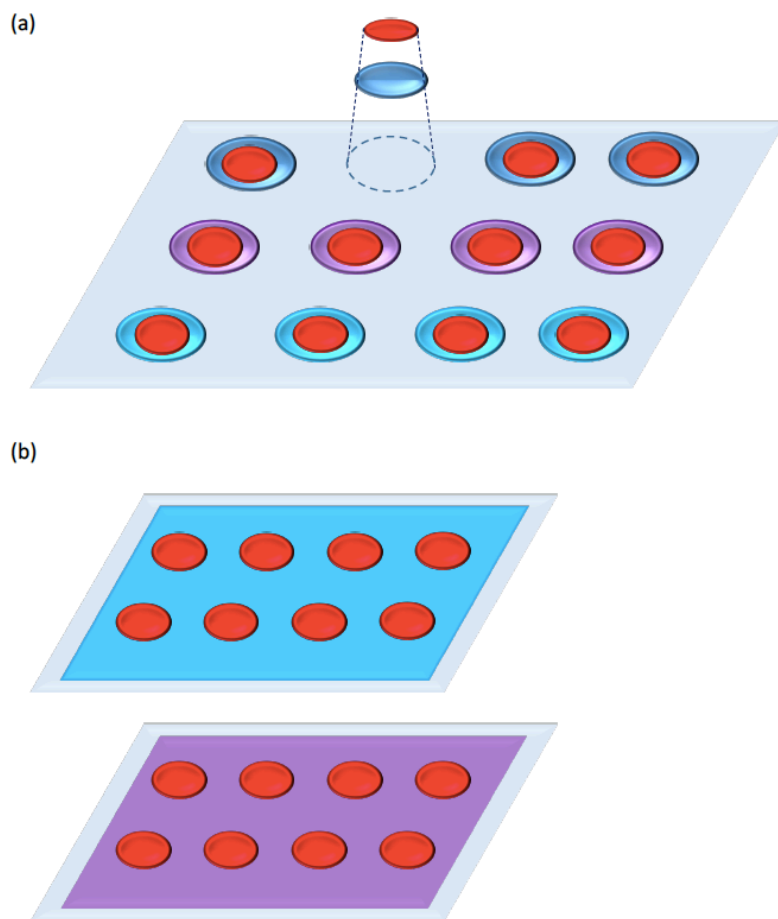


Figure 4: Spotted polymers technique (a) and flat coating technique (b).

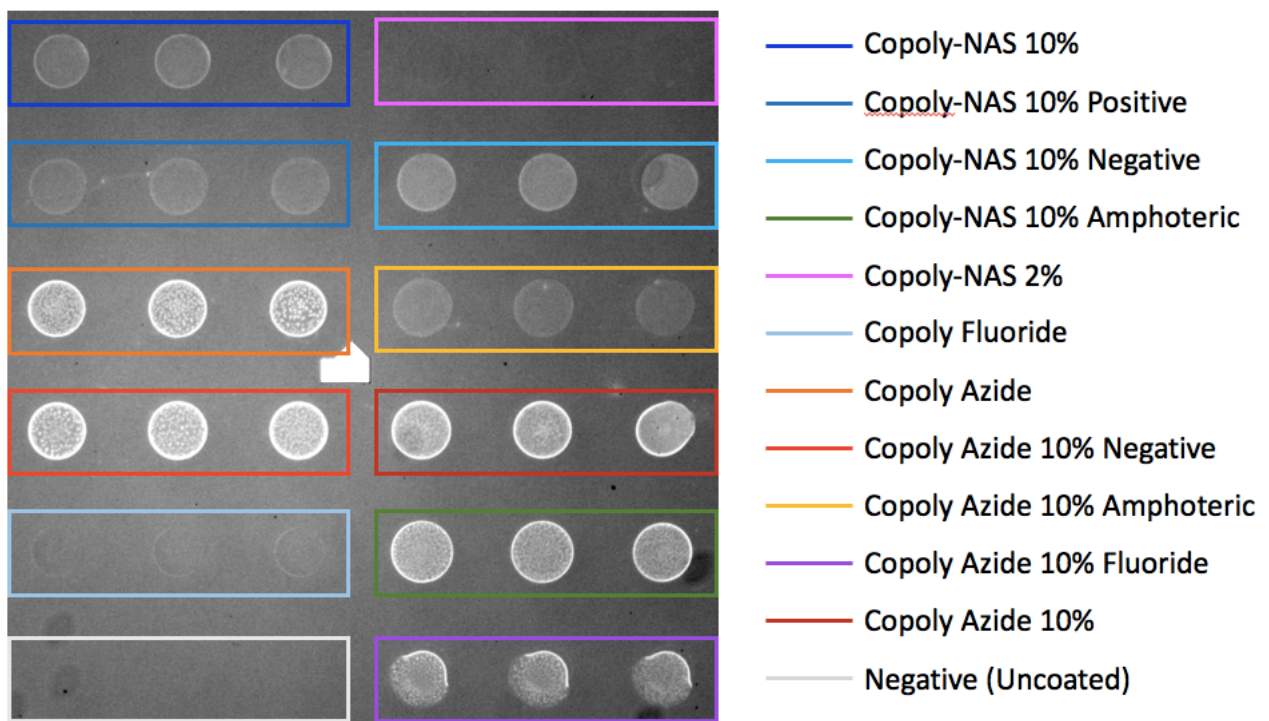


Figure 5 – Dry IRIS chip image acquired before starting the real-time binding experiment. On the chip a 6x6 matrix of  $\alpha$ -lactalbumin spots is visible. Each group of three spots corresponds to a different polymer.

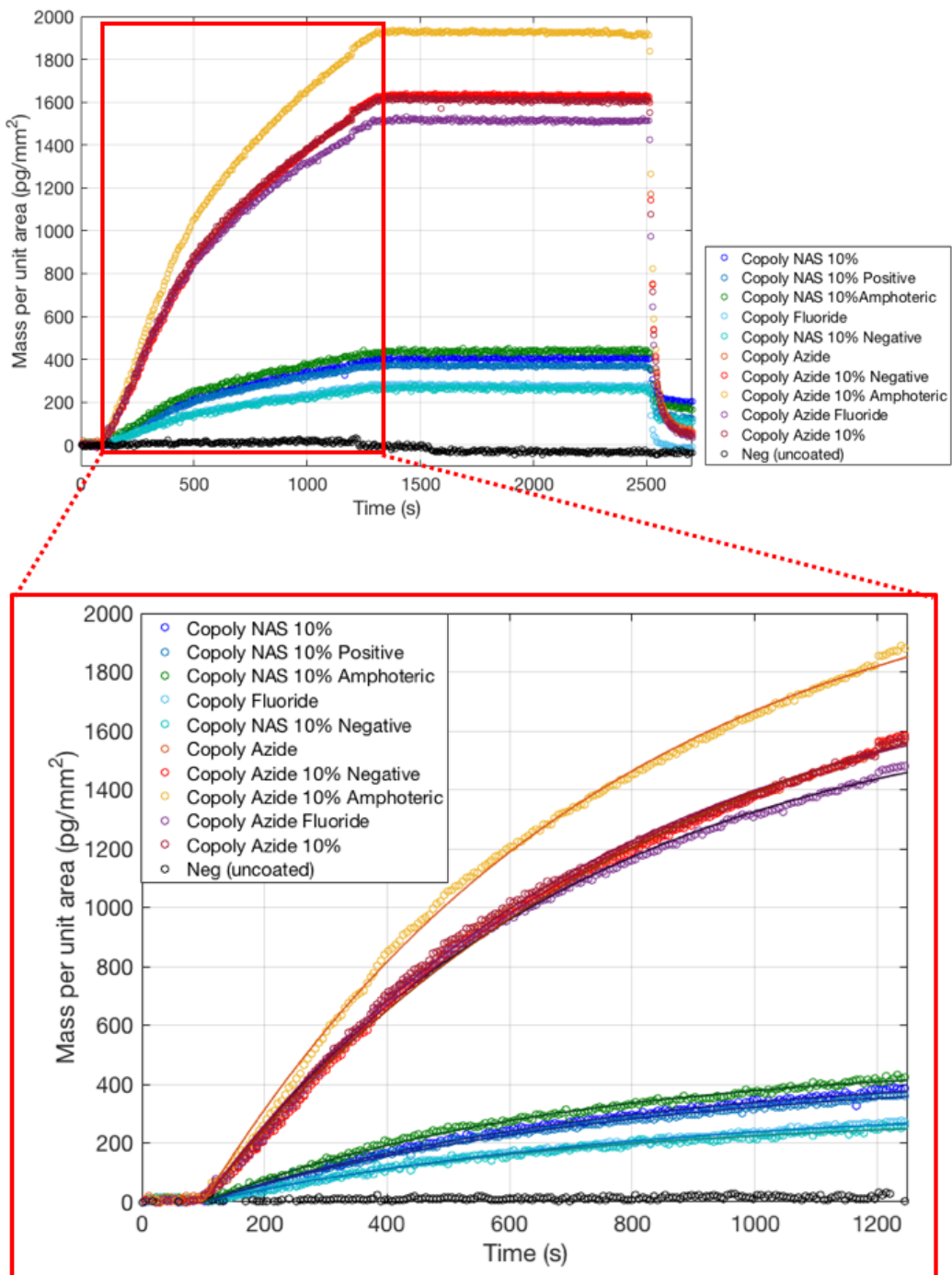


Figure 6: Anti-  $\alpha$ -lactalbumin binding to two different modifications of  $\alpha$ -lactalbumin spotted on a single IRIS chip. The solid lines in the inset (a) show a classic Langmuir fit of the data.

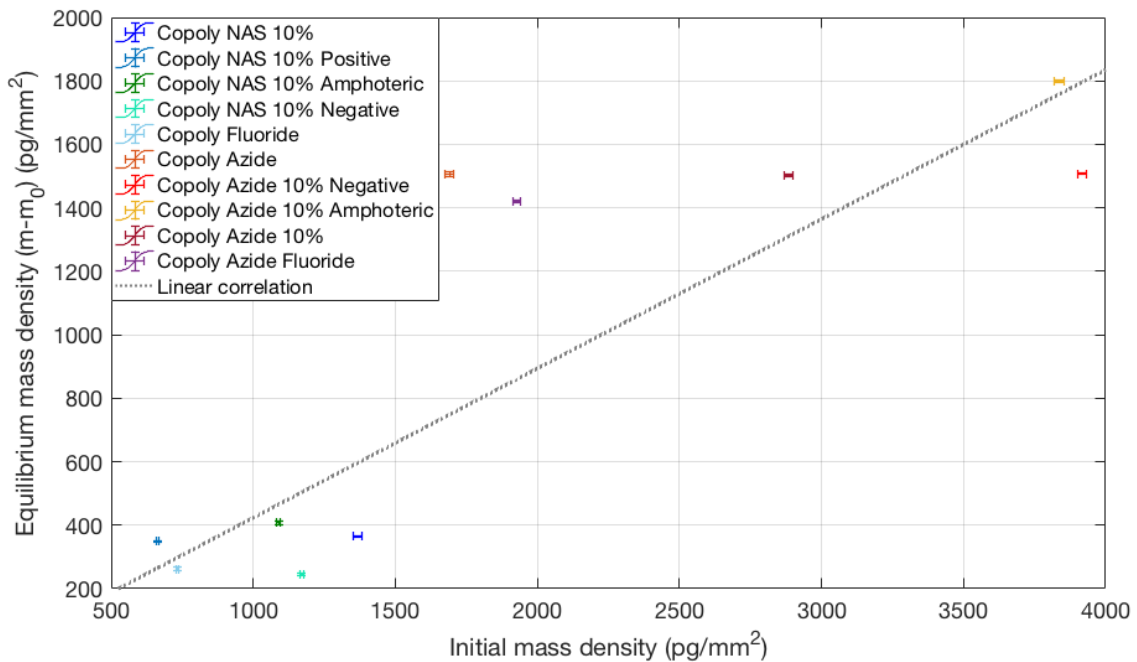


Figure 7 – Correlation between the initial mass density value and the equilibrium value reached by the antibody binding to different polymer spots.

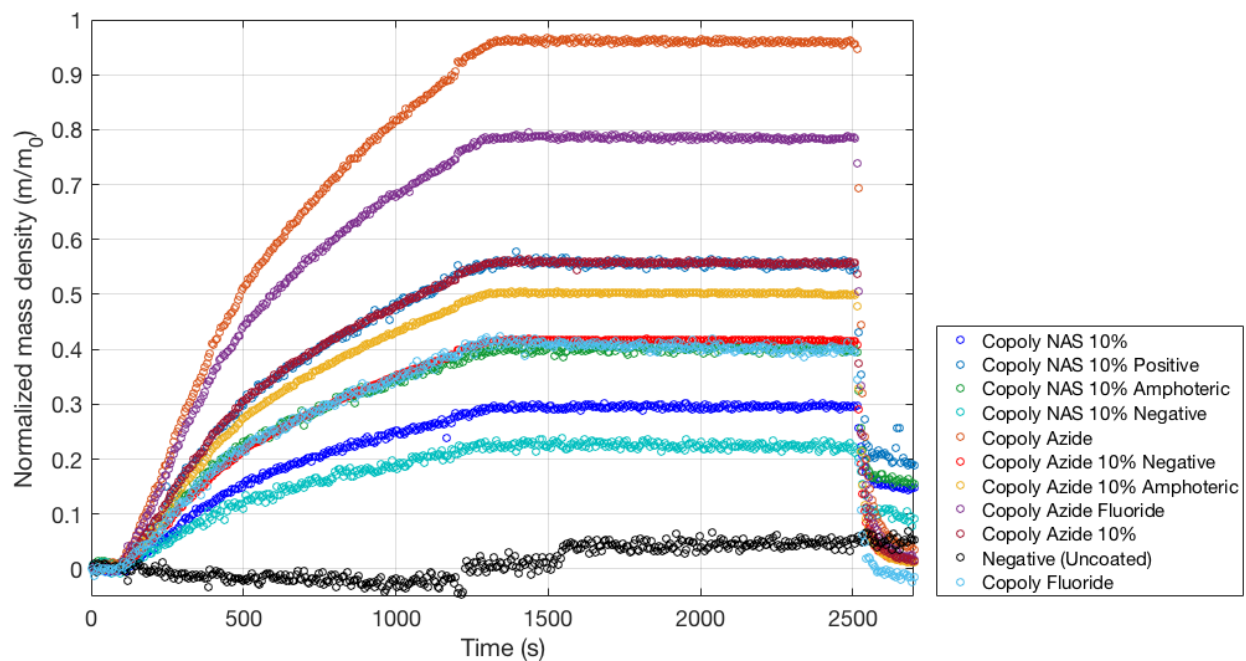


Figure 8: The curves in figure 6a, normalized by dividing every curve for the initial mass value.

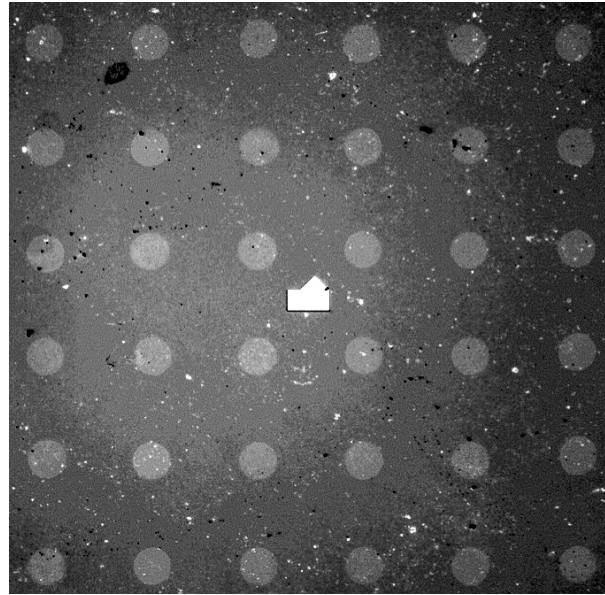
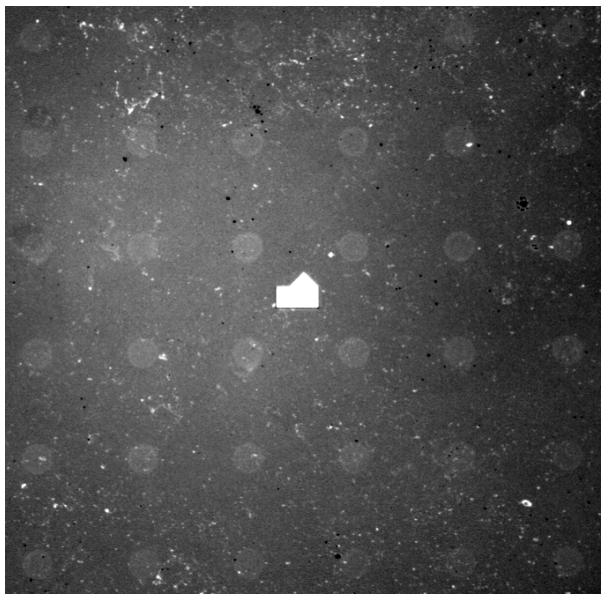


Figure 9 – Dry IRIS chip images acquired before starting the real-time binding experiment. (a) Copoly-10F coated chip and (b) MCP-4 amphoteric coated chip. On both a 6x6 matrix of  $\alpha$ -lactalbumin spots is visible.

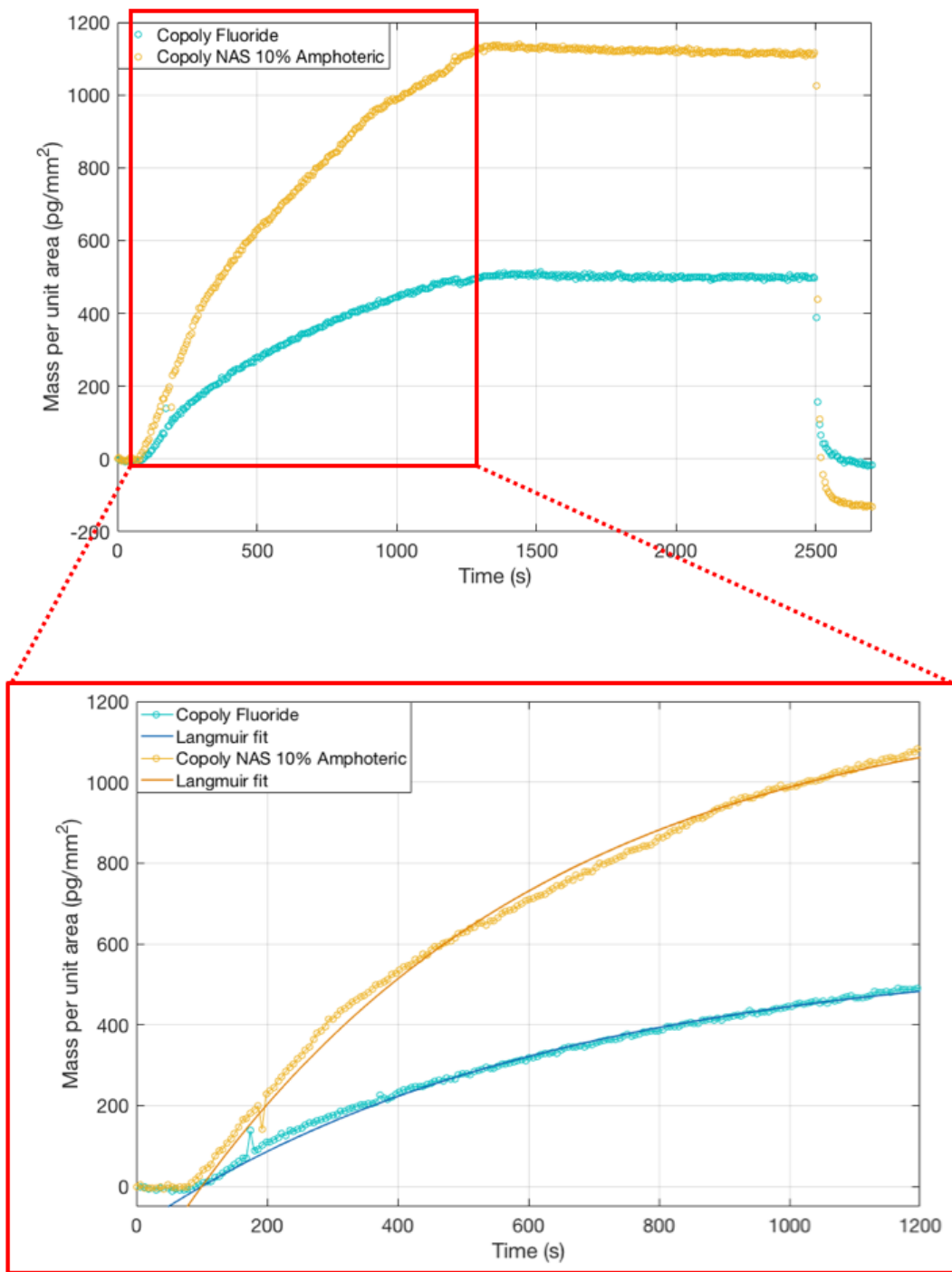


Figure 10: Anti- $\alpha$ -lactalbumin binding to  $\alpha$ -lactalbumin spotted on two flat-coated IRIS chips: one coated with Copoly Fluoride (light blue curve) and one with Copoly NAS 10% Amphoteric (yellow). The solid lines in the inset (a) show a classic Langmuir fit of the data.

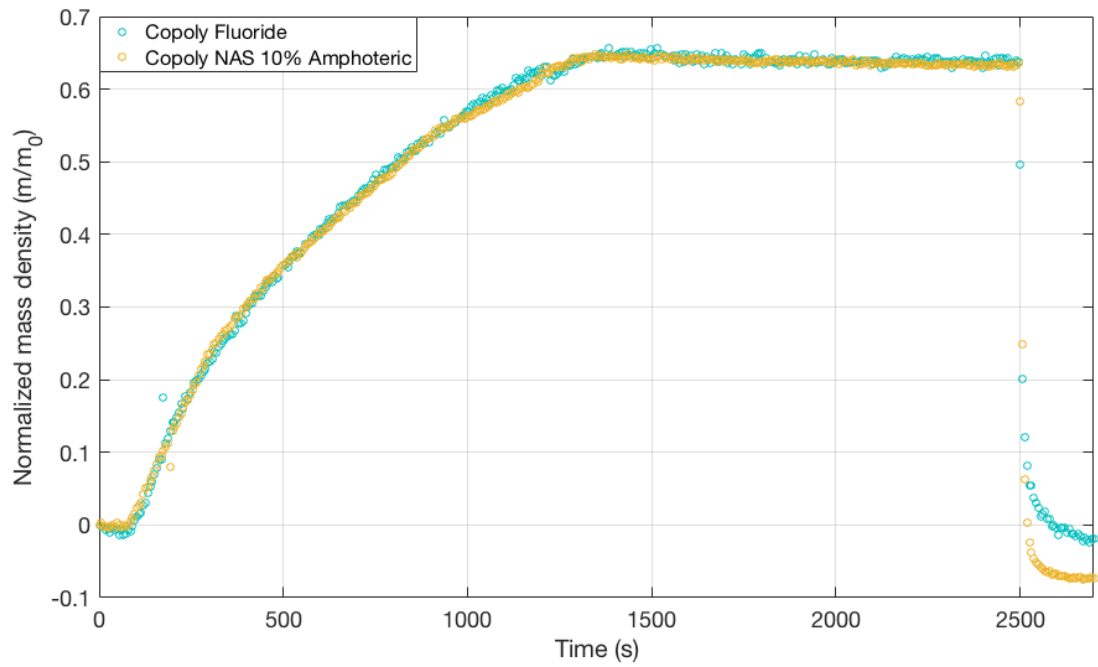


Figure 11: The curves in Figure 10, normalized by dividing each of them by the initial mass density value.

Tables:

Copolymer	Monomer mole percent				
	m	n	p	q	o
Copoly NAS 10%	89	10	1	-	-
Copoly NAS 10% positive	87	10	1	2	-
Copoly NAS 10% negative	87	10	1	2	-
Copoly NAS 10% amphoteric	87.5	10	0.5	1	1
Copoly Fluoride	94	2	1	3	-
Copoly Azide	97	2	1	-	-
Copoly Azide 10%	89	10	1	-	-
Copoly Azide 10% negative	87	10	1	2	-
Copoly Azide 10% amphoteric	87.5	10	0.5	1	1
Copoly Azide Fluoride	94	2	1	3	-

Table 1: Molar ratio of monomers used to synthesize polymers.

Copolymer	$k_{ON} (M^{-1}s^{-1})$	$k_{OFF} (s^{-1})$	$K_D (M)$
Copoly NAS 10%	$(9.4 \pm 0.2) \cdot 10^4$	$(7.2 \pm 0.1) \cdot 10^{-4}$	$(0.77 \pm 0.02) \cdot 10^{-8}$
Copoly NAS 10% positive	$(9.0 \pm 0.1) \cdot 10^4$	$(7.7 \pm 0.3) \cdot 10^{-4}$	$(0.86 \pm 0.04) \cdot 10^{-8}$
Copoly NAS 10% negative	$(8.3 \pm 0.2) \cdot 10^4$	$(9.7 \pm 0.6) \cdot 10^{-4}$	$(1.17 \pm 0.08) \cdot 10^{-8}$
Copoly NAS 10% amphoteric	$(11.1 \pm 0.2) \cdot 10^4$	$(6.5 \pm 0.1) \cdot 10^{-4}$	$(0.59 \pm 0.01) \cdot 10^{-8}$
Copoly Fluoride	$(6.5 \pm 0.1) \cdot 10^4$	$(8.8 \pm 0.4) \cdot 10^{-4}$	$(1.35 \pm 0.07) \cdot 10^{-8}$
Copoly Azide	$(7.7 \pm 0.1) \cdot 10^4$	$(8.4 \pm 0.3) \cdot 10^{-4}$	$(1.09 \pm 0.04) \cdot 10^{-8}$
Copoly Azide 10% negative	$(7.5 \pm 0.7) \cdot 10^4$	$(7.8 \pm 0.2) \cdot 10^{-4}$	$(1.04 \pm 0.10) \cdot 10^{-8}$
Copoly Azide 10% amphoteric	$(9.6 \pm 0.9) \cdot 10^4$	$(8.2 \pm 0.3) \cdot 10^{-4}$	$(0.85 \pm 0.09) \cdot 10^{-8}$
Copoly Azide 10% Fluoride	$(8.0 \pm 0.8) \cdot 10^4$	$(9.0 \pm 0.3) \cdot 10^{-4}$	$(1.13 \pm 0.12) \cdot 10^{-8}$
Copoly Azide 10%	$(9.8 \pm 0.1) \cdot 10^4$	$(8.8 \pm 0.2) \cdot 10^{-4}$	$(1.00 \pm 0.03) \cdot 10^{-8}$

Table 2: ON and OFF rates obtained through a classic Langmuir fit of anti-  $\alpha$ -lactalbumin binding on different alpha-lactalbumin modifications, spotted on top of different polymers spots.

Copolymer	Initial mass density (ng/mm <sup>2</sup> )
Copoly NAS 10%	$1.36 \pm 0.2$
Copoly NAS 10% positive	$0.66 \pm 0.2$
Copoly NAS 10% negative	$1.17 \pm 0.3$
Copoly NAS 10% amphoteric	$1.09 \pm 0.6$
Copoly Fluoride	$0.73 \pm 0.4$
Copoly Azide	$1.69 \pm 0.7$

<b>Copoly Azide 10% negative</b>	$3.92 \pm 0.3$
<b>Copoly Azide 10% amphoteric</b>	$3.83 \pm 0.4$
<b>Copoly Azide 10% Fluoride</b>	$2.89 \pm 0.4$
<b>Copoly Azide 10%</b>	$1.93 \pm 0.3$
<b>Negative (Uncoated)</b>	$-0.69 \pm 0.5$

Table 3: Initial mass density values for the different polymers spots.

COPOLYMER	$k_{ON} (M^{-1}s^{-1})$	$k_{OFF}(s^{-1})$	$K_D(M)$
<b>Copoly Fluoride</b>	$(1.37 \pm 0.02) \cdot 10^4$	$(1.59 \pm 0.04) \cdot 10^{-3}$	$(11.6 \pm 0.4) \cdot 10^{-8}$
<b>Copoly NAS 10% amphoteric</b>	$(2.99 \pm 0.05) \cdot 10^4$	$(1.44 \pm 0.04) \cdot 10^{-3}$	$(4.8 \pm 0.2) \cdot 10^{-8}$

Table 4: ON and OFF rates obtained through a classic Langmuir fit of anti-  $\alpha$  -lactalbumin binding on spotted Copoly Fluoride (blue curve, fig.4a) and on spotted Copoly NAS 10% amphoteric (yellow curve, fig.4a).

Copolymer	Spotted initial mass density (ng/mm <sup>2</sup> )	Flat-coated initial mass density (ng/mm <sup>2</sup> )
<b>Copoly NAS 10% amphoteric</b>	$1.09 \pm 0.6$	$1.76 \pm 0.2$
<b>Copoly Fluoride</b>	$0.73 \pm 0.4$	$0.78 \pm 0.1$

Table 5 – Comparison of the initial mass density value for Copoly Fluoride and Copoly NAS 10% amphoteric polymers for the two experiments.